

# Higgs boson production at Linear Colliders from a generic 2HDM: the role of triple Higgs self-interactions

David López-Val<sup>1</sup>, Joan Solà<sup>2</sup>

<sup>1</sup>Institut für Theoretische Physik, Universität Heidelberg  
Philosophenweg 16, 67119 Heidelberg, Germany.

<sup>2</sup>High Energy Physics Group, Dept. ECM, and Institut de Ciències del Cosmos  
Universitat de Barcelona  
Av. Diagonal 647, E-08028 Barcelona, Catalonia, Spain.

We review selected results for Higgs boson production at Linear Colliders in the framework of the general Two-Higgs-Doublet Model (2HDM). We concentrate on the analysis of i) the pairwise production of neutral Higgs bosons ( $h^0 A^0, H^0 A^0$ ); and ii) the neutral Higgs boson-strahlung modes ( $h^0 Z^0, H^0 Z^0$ ). We identify sizable production rates, in the range of  $\sigma \sim \mathcal{O}(10 - 100)$  fb for  $\sqrt{s} = 0.5$  TeV, alongside with large quantum effects ( $\delta_r \sim \pm 50\%$ ), which we can fundamentally track down to the enhancement power of the triple-Higgs self-interactions. This constitutes a telltale signature of the 2HDM, with no counterpart in e.g. the Minimal Supersymmetric Standard Model (MSSM). We compare these results with several complementary double and triple  $\mathcal{O}(\alpha_{ew}^3, \alpha_{ew}^4)$  Higgs-boson production mechanisms and spotlight a characteristic phenomenological profile which could eventually be highly distinctive of a non-supersymmetric two-Higgs-doublet structure.

## 1 Introduction

Deciphering the fundamental nature of Electroweak Symmetry Breaking (EWSB) lies at the very frontline of the current theoretical and experimental research in Particle Physics. Even in spite of the tantalizing Higgs boson candidates recently identified by the ATLAS and CMS experiments [1], a long way might yet stand ahead of us until we are able to convincingly close in on such a longstanding conundrum. In particular, were these signatures finally confirmed, a first question to be answered would be whether they can be described within the minimal framework of the Standard Model (SM) or, on the contrary, if they should rather be attributed to an extended EWSB sector [2]. One canonical example of the latter is the general Two-Higgs-Doublet Model (2HDM) [3]. The model is built upon a second scalar  $SU_L(2)$  doublet with  $Y = +1$  weak hypercharge. This results into a larger Higgs boson spectrum of five physical Higgs fields: neutral  $CP$ -even ( $h^0, H^0$ ), neutral  $CP$ -odd ( $A^0$ ) and charged  $H^\pm$ . Such a simple, but yet non-minimal extension of the SM Higgs sector has gathered growing attention over the past years [4] and become a cherished setup for model builders and phenomenologists alike. Besides the many novel, and usually highly distinctive features put forward by the model in multifarious domains – from collider to flavor physics or astrophysics –, the 2HDM provides a suitable low-energy description to many UV completions of the the EWSB dynamics.

The model is fully specified once we fix i) the masses of the physical Higgs bosons; ii) the ratio  $\tan\beta \equiv \langle H_2^0 \rangle / \langle H_1^0 \rangle$  of the two Vacuum Expectation Values (VEVs) giving masses to the up- and down-like quarks; iii) the mixing angle  $\alpha$  between the two  $CP$ -even states; and iv) one remaining Higgs boson self-coupling in the Higgs potential, hereafter dubbed  $\lambda_5$ . We note in passing that the Higgs sector of the MSSM [5] corresponds to a particular realization of the general (unconstrained) 2HDM, for which the invariance under SUSY transformations enforces a number of additional restrictions – most significantly, the Higgs boson self-interactions become tied to the gauge couplings. This situation is remarkably different in the general 2HDM, where the size of these self-interactions is fundamentally unrestricted and it only becomes limited, in practice, by the interplay of theoretical consistency conditions (unitarity [6], vacuum stability [7]) and experimental bounds (viz. the excluded Higgs boson mass ranges from the from direct collider searches,

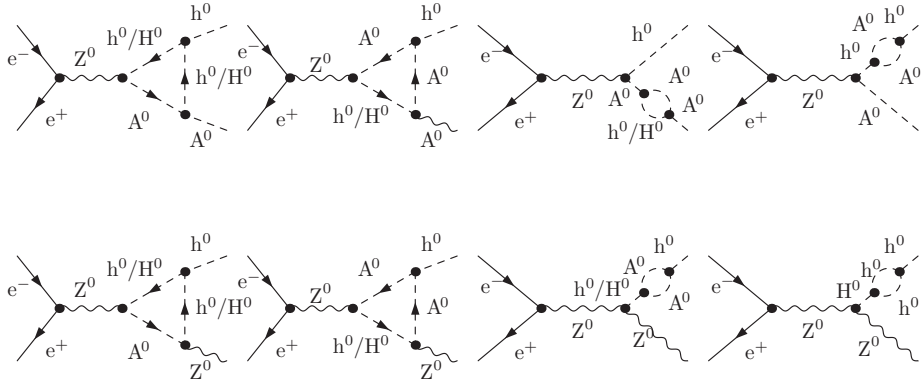


Figure 1: Sample of one-loop Higgs-mediated Feynman diagrams which account for the bulk of the quantum effects to the neutral Higgs pair  $e^+e^- \rightarrow h^0 A^0$  (upper row) and the Higgs-strahlung mechanisms  $e^+e^- \rightarrow h^0 Z^0$  (lower row).

and also the constraints derived from electroweak [8] and flavor physics observables [9]). A detailed account of these restrictions and of the model setup can be found in Ref. [10]. For comprehensive analyses of the 2HDM parameter space constraints, see e.g. Refs. [11].

Following the eventual discovery of the Higgs boson(s) at the LHC, it will be crucial to address the precise experimental determination of the corresponding quantum numbers, mass spectrum and couplings to other particles. A linear collider (linac) can play a central role in this enterprise [12]. Dedicated studies have exhaustively scrutinized the phenomenological imprints of the basic 2HDM Higgs boson production modes, such as e.g. i) triple Higgs,  $e^+e^- \rightarrow 3h$  [13]; ii) inclusive Higgs-pair through EW gauge boson fusion,  $e^+e^- \rightarrow V^*V^* \rightarrow 2h + X$  [14]; iii) exclusive Higgs-pair  $e^+e^- \rightarrow 2h$  [10, 15]; and iv) Higgs strahlung, or associated production with a weak gauge boson  $e^+e^- \rightarrow hV$  [16], with  $[h \equiv h^0, A^0, H^0, H^\pm]$  and  $[V \equiv Z^0, W^\pm]^1$ . As a common highlight, all these studies report on sizable production rates and large quantum effects, arising from the potentially enhanced Higgs self-interactions. Interestingly enough, Higgs boson searches at  $e^+e^-$  colliders may also benefit from alternative running modes, particularly from  $\gamma\gamma$  scattering. Processes such as  $\gamma\gamma$ -induced production of single ( $\gamma\gamma \rightarrow h$ ) and double ( $\gamma\gamma \rightarrow 2h$ ) Higgs bosons have been studied from this viewpoint. These entirely operate at the quantum level, via an effective (loop-induced) Higgs/photon interaction  $g_{\gamma\gamma h}$  that we may regard as a direct probe of non-standard (charged) degrees of freedom coupled to the Higgs sector. The aforementioned single Higgs channels have been considered in the framework of the SM [18], the 2HDM [19] and the MSSM [20, 21] and are known to exhibit excellent experimental prospects, not only due to the clean environment inherent to a linac machine, but also owing to the high attainable  $\gamma\gamma$  luminosity, and the possibility to tune the  $\gamma$ -beam polarization as a strategy to enlarge the signal-versus-background ratios<sup>2</sup>.

## 2 Numerical analysis

In this contribution we review two particular 2HDM Higgs boson production modes at a linear collider, to wit: i) the pairwise production of neutral Higgs bosons  $e^+e^- \rightarrow h^0 A^0/H^0 A^0$ ; and ii) the associated production of a neutral Higgs and a  $Z^0$  bosons,  $e^+e^- \rightarrow h^0 Z^0/H^0 Z^0$  – the so-called Higgs-strahlung mechanism, which we can regard as the 2HDM analog(s) to the Bjorken process in the SM [23]. The motivation herewith is threefold: i) a first focus point is to seek for the most favorable regions across the 2HDM parameter space, for which the Higgs boson production rates become optimal, and to correlate them to alternative multi-Higgs production modes; ii) second, we aim at quantifying the importance of the radiative corrections associated to these processes; iii) and third, we shall examine the impact of the Higgs boson self interactions and their

<sup>1</sup>For related work in the context of MSSM Higgs boson production see e.g. [17].

<sup>2</sup>Analogue studies for the  $\gamma\gamma \rightarrow hh$  mode are available e.g. in Ref. [22].

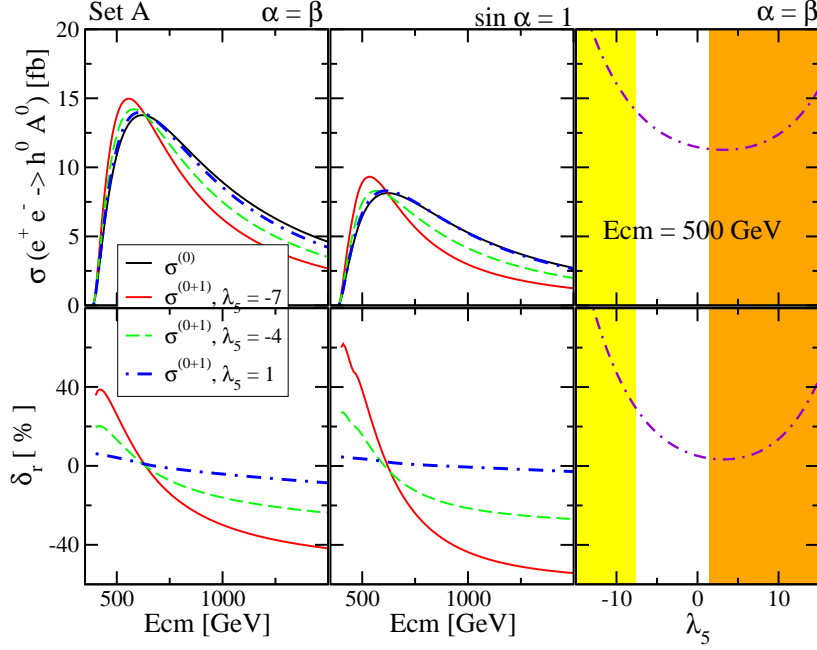


Figure 2: Tree-level and loop-corrected cross section  $[\sigma(e^+e^- \rightarrow h^0 A^0)]$  (in fb), alongside with the relative size of the radiative corrections  $[\delta_r \equiv [\sigma^{(0+1)} - \sigma^{(0)}]/\sigma^{(0)}]$  (in %), as a function of  $\sqrt{s}$  (left, center) and  $\lambda_5$  (right). We fix  $\tan\beta = 1.2$  (compatible with the lower  $\tan\beta$  bound from  $B_d^0 - \bar{B}_d^0$  data [9]) and examine the representative choices  $\alpha = \beta$  (maximum  $g_{h^0 A^0 Z^0}$  tree-level coupling) and  $\alpha = \pi/2$  (fermiophobic limit for  $h^0$  in type-I 2HDM). The influence of the Higgs self-interactions is assessed by dialing the value of the parameter  $\lambda_5$ . The shaded areas on the left (resp. right) are excluded by unitarity (resp. vacuum stability).

potentially enhanced strength. The leading order production rates merely depend on the Higgs couplings to the Z boson. In other words, they are entirely subdued by the gauge symmetry – and hence they feature no disclosing scenarios between the general 2HDM and e.g. the MSSM. The resulting phenomenological portrayal, however, may clearly depart once the quantum effects to such couplings are considered. Vertex corrections, in particular, turn out to be sensitive to the triple Higgs self-interactions through the interchange of virtual Higgs bosons which are then linked to the external Higgs boson legs. A sample of such Higgs-mediated one-loop diagrams is displayed in Fig. 1. These effects we can roughly describe by a loop-induced form factor, which spells out how the strength of the bare Higgs-to-gauge boson couplings is modified:

$$g_{hA^0 Z^0} \rightarrow g_{hA^0 Z^0} \left[ 1 + \frac{|\lambda_{HHH}|^2}{16\pi^2 s} f(M_h^2/s, M_{A^0}^2/s) \right]. \quad (1)$$

Here  $\lambda_{HHH}$  stands for generic triple Higgs self-interaction, and  $1/16\pi^2$  for the standard loop integral suppression factor. By  $f(M_h^2/s, M_{A^0}^2/s)$  we denote a generic rational function involving the ratios of the different mass scales taking part in the process. The above expression (1) indicates how the Higgs-to-gauge boson couplings, which are entirely anchored by the gauge symmetry at the leading-order, may be strongly promoted at one-loop through the indirect effect of the Higgs boson self-couplings – unlike their MSSM counterparts.

## 2.1 Calculational setup

Throughout our study we make use of the standard algebraic and numerical packages FEYNARTS, FORMCALC and LOOPTOOLS [24]. Updated experimental constraints (from EW precision data, low-energy flavor-physics and the Higgs mass regions ruled out by direct collider searches), as well as theoretical consistency

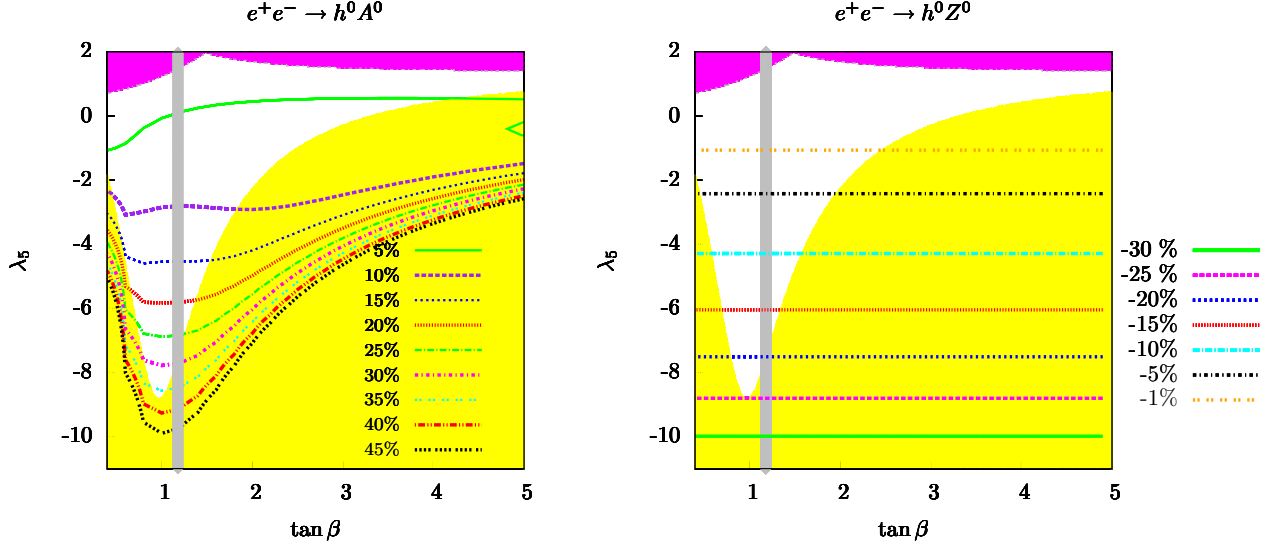


Figure 3: Contour plots for the relative size of the one-loop quantum corrections  $\delta_r \equiv [\sigma^{(0+1)} - \sigma^{(0)}]/\sigma^{(0)}$  (in %) to the  $e^+e^- \rightarrow h^0 A^0$  (left panel) and  $e^+e^- \rightarrow h^0 Z^0$  (right panel) total rates, as a function of  $\tan \beta$  and  $\lambda_5$ . We fix  $\alpha = \beta$  (for  $e^+e^- \rightarrow h^0 A^0$ ) and  $\alpha = \beta - \pi/2$  (for  $e^+e^- \rightarrow h^0 Z^0$ ), in which cases their respective born-level couplings maximize. For the Higgs boson masses we use Set A from Tab. 1. The linac center-of-mass energy is taken to be  $\sqrt{s} = 500$  GeV. The shaded areas in the upper (resp. lower) patches of the  $\tan \beta - \lambda_5$  plane are excluded by unitarity [6] (resp. vacuum stability [7]) bounds. The vertical grey strip accounts for the lower limit  $\tan \beta \simeq 1.18$  stemming from  $B_d^0 - \bar{B}_d^0$  data [9].

conditions (perturbativity, unitarity and vacuum stability) are duly taken into account [6, 7, 9, 11, 25, 26]. For definiteness, we set along two Higgs boson mass benchmark choices A and B, as quoted in Tab. 1:

	$M_{h^0}$ [GeV]	$M_{H^0}$ [GeV]	$M_{A^0}$ [GeV]	$M_{H^\pm}$ [GeV]
Set A	130	200	260	300
Set B	130	150	200	160

Table 1: Choices of Higgs boson masses employed throughout our calculation.

In order to carry out the complete one-loop computation we are entitled to define suitable UV counterterms, in particular for the renormalization of the Higgs boson masses and wave functions. These we can express in terms of the Higgs 2-point functions at order  $\mathcal{O}(\alpha_{ew})$ . Conventional on-shell renormalization conditions – see e.g. Ref. [27] – are extended to the 2HDM Higgs sector. In particular, the relations

$$\left. \text{Re } \hat{\Sigma}'_{A^0 A^0}(q^2) \right|_{q^2=M_{A^0}^2} = 0; \quad \left. \text{Re } \hat{\Sigma}_{A^0 Z^0}(q^2) \right|_{q^2=M_{A^0}^2} = 0,$$

anchor the wave function renormalization of the Higgs doublets, and thereby of all the physical Higgs fields. The remaining Higgs boson masses, as well as the mixing angle  $\alpha$ , are determined via on-shell conditions imposed on their respective self-energies (including the  $h^0 - H^0$  kinetic mixing). The parameter  $\tan \beta$  is fixed via Eq. (2) alongside with one additional condition on the Higgs boson tadpoles. An exhaustive account of the renormalization procedure is available in Ref. [10].

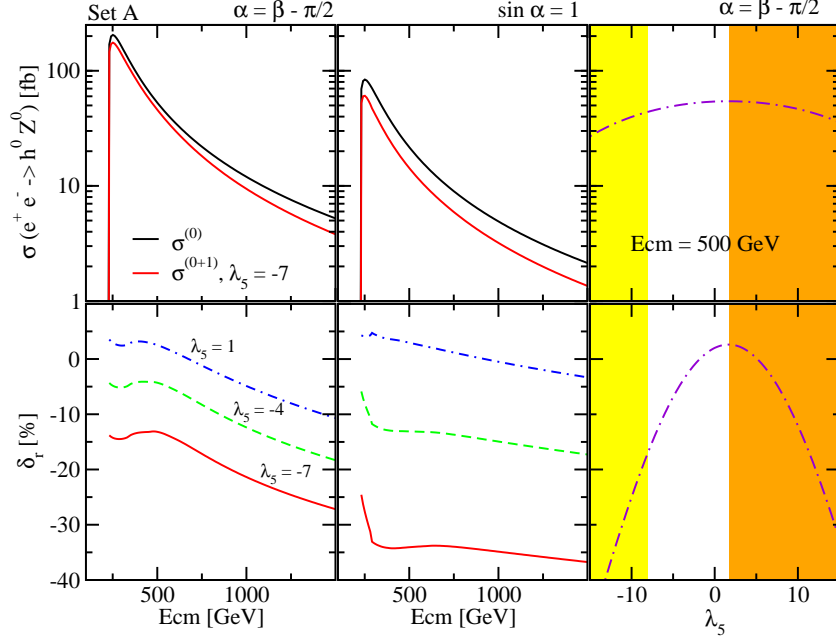


Figure 4: Tree-level and loop-corrected cross section [ $\sigma(e^+e^- \rightarrow h^0 A^0)$ ] (in fb) and relative size of the radiative corrections [ $\delta_r$ ] (in %), as a function of  $\sqrt{s}$  (left, center) and  $\lambda_5$  (right), for an equivalent setup to that of Fig. 2.

## 2.2 Higgs boson pair production at $\mathcal{O}(\alpha_{ew}^3)$ : $e^+e^- \rightarrow h^0 A^0/H^0 A^0$

For definiteness, we focus on the light Higgs mode [ $h^0 A^0$ ] and specialize our results for the Higgs mass spectrum defined by Set A of Tab. 1. We quantify our analysis by means of i) the Born-level, [ $\sigma^{(0)}$ ], and 1-loop cross sections, [ $\sigma^{(0+1)}$ ] – in which we include the full set of  $\mathcal{O}(\alpha_{ew}^3)$  corrections, and also the leading  $\mathcal{O}(\alpha_{ew}^4)$  ones which arise from the squared of the scattering amplitude [10]; ii) the relative size of the 1-loop corrections, via the parameter  $\delta_r \equiv [\sigma^{(0+1)} - \sigma^{(0)}]/\sigma^{(0)}$ . The upshot of our findings, as summarized in Fig. 2, highlights substantial production rates, which fall roughly in the range of 2 – 15 fb for  $\sqrt{s} = 0.5$  TeV – this is, up to barely  $10^3 - 10^4$  events per 500 fb $^{-1}$ ; and eventually very large quantum corrections, of the order  $|\delta\sigma|/\sigma \sim 20 - 60\%$ , which can be either positive (for  $\sqrt{s} \simeq 0.5$  TeV) or negative ( $\sqrt{s} \gtrsim 1$  TeV) and fairly independent on the details of the Higgs mass spectrum, the particular value of the tree-level coupling [ $g_{hA^0 Z}$ ] and the actual type of 2HDM under consideration – namely, whether we specifically target at the type-I or II realizations of the 2HDM. The evolution of  $\sigma^{(0+1)}$  and  $\delta_r$  as a function of  $\sqrt{s}$  for different  $\lambda_5$  values evinces how critically the quantum effects depend on the Higgs self-interaction enhancements. The quadratic dependence on the parameter  $\lambda_5$ ,  $\sigma \sim (a - b\lambda_5)^2$ , as shown in the rightmost panel of Fig. 2, nicely illustrates the dominance of the Higgs mediated one-loop diagrams – these are indeed sensitive to the product of two triple Higgs self-interactions. As a complementary viewpoint, in the left panel of Fig. 3 we display the profile of the radiative corrections  $\delta_r$  to the total cross-section [ $\sigma(h^0 A^0)$ ] along the  $\tan\beta - \lambda_5$  plane, again for Set A of Higgs boson masses,  $\alpha = \beta$  and a linac center-of-mass energy of  $\sqrt{s} = 0.5$  TeV. The choice  $\alpha = \beta$  maximizes the tree-level cross section. Unitarity [6] and vacuum stability limits [7] (lower and upper shaded areas, respectively) restrict the largest attainable quantum effects to regions with  $\tan\beta \simeq 1$  and  $|\lambda_5| \sim 5 - 10$  ( $\lambda_5 < 0$ ). The central grey band depicts the lower limit  $\tan\beta \simeq 1.18$  ensuing from  $B_d^0 - \bar{B}_d^0$  [9].

## 2.3 Associated Higgs/ $Z^0$ -boson production at $\mathcal{O}(\alpha_{ew}^3)$ : $e^+e^- \rightarrow h^0 Z^0/H^0 Z^0$

Again, without loss of generality, we concentrate on the light Higgs mode [ $h^0 Z^0$ ] and arrange the mass spectrum as in Set A of Tab. 1. Our results are shown in Fig. 4. In this case we obtain typical cross sections

Process	$\sigma(\sqrt{s} = 0.5 \text{ TeV})[\text{fb}]$	$\sigma(\sqrt{s} = 1.0 \text{ TeV})[\text{fb}]$	$\sigma(\sqrt{s} = 1.5 \text{ TeV})[\text{fb}]$
$h^0 A^0$	26.71 ( $\delta_r = 31.32\%$ )	4.07	1.27
$H^0 Z^0$	19.09 ( $\delta_r = -61.56\%$ )	3.73	1.47
$h^0 H^0 A^0$	0.02	5.03	3.55
$H^0 H^+ H^-$	0.17	11.93	8.39
$h^0 h^0 + X$	1.47	17.36	38.01

Table 2: Compared cross section (in fb) for different associated, pairwise and triple Higgs boson production mechanisms at  $\mathcal{O}(\alpha_{ew}^3, \alpha_{ew}^4)$ , for  $\tan\beta = 1$ ,  $\alpha = \beta$  and  $\lambda_5 = -10$ . The Higgs boson mass spectrum we fix as in Set B of Tab. 1. The relative size of the one-loop corrections  $[\delta_r]$  for the Higgs pair and Higgs strahlung mechanisms is quoted in brackets.

in the range of  $\sigma(h^0 Z^0) \sim \mathcal{O}(10 - 100) \text{ fb}$ , with very significant (and systematically negative) radiative corrections (up to order  $\delta_r \sim -50\%$ ), reaching their maximum again in the parameter space regions with  $\tan\beta \sim \mathcal{O}(1)$  and  $|\lambda_5| \sim \mathcal{O}(10)$ . Such a characteristic pattern of negative quantum effects we can relate to the dominance of the finite wave function corrections to the external Higgs boson fields – this being the only contribution which retains a quadratic dependence on  $\lambda_{HHH}$  at one loop, as we can also read off the rightmost panel of Fig. 4. The relative size of the quantum effects  $[\delta_r]$  and its interplay with the relevant constraints is examined in the right panel of Fig. 3 as we move across the  $\tan\beta - \lambda_5$  plane. Set A of Higgs boson masses, a fixed value of  $\alpha = \beta - \pi/2$  and a linac center-of-mass energy to  $\sqrt{s} = 0.5 \text{ TeV}$  are employed throughout. Worth noticing is that the  $\delta_r$  isocurves are not responsive to a change of  $\tan\beta$ . This follows directly from the analytical structure of all the relevant couplings for the particular setup  $\alpha = \beta - \pi/2$  [16] – which corresponds to the decoupling (or SM-like) limit of the 2HDM.

### 3 Discussion and closing remarks

Higgs boson self-interactions constitute a paradigmatic structure of extended Higgs sectors of non-supersymmetric nature. The general (unconstrained) Two-Higgs-Doublet Model is a canonical example of the latter. Here, the triple and quartic Higgs boson self-interactions are not subdued by the gauge symmetry. This entails two major consequences, which are in stark contrast to analogue models, such as e.g. the MSSM: i) the Higgs boson spectrum is fully unconstrained; this is to say, no limitations on the mass splittings between the physical Higgs boson fields must be assumed *a priori*; ii) by the very same token, the Higgs boson self interactions are also fundamentally unrestricted, and hence may accomodate sizable enhancements. Both features are tamed in part by stringent theoretical and phenomenological constraints (unitarity, vacuum stability, electroweak precision and flavor physics) but nevertheless open up a plethora of rich, and highly distinctive, phenomenological possibilities. So much so, the analysis of collider observables which are sensitive to the Higgs self-interactions, either directly or through quantum corrections, may bring forward instrumental handles to disclose non-SUSY vs SUSY multi-doublet Higgs structures.

In this contribution we have concisely revisited two particular examples of Higgs boson production from  $e^+e^-$  colliders within the 2HDM context, these are the pairwise production of neutral Higgs bosons ( $h^0 A^0/H^0 A^0$ ) and the Higgs-strahlung channels ( $h^0 Z^0/H^0 Z^0$ ). We have portrayed their phenomenology at a future linac and have spelled out the features that singularize the 2HDM scenarios with large Higgs boson self-couplings. Our findings can be outlined as follows:

- **Large Higgs boson production rates**, in the ballpark of  $\sigma_{2h,hZ} \sim \mathcal{O}(10 - 100) \text{ fb}$  for  $\sqrt{s} = 500 \text{ GeV}$ , and yet of few dozens of fb in the TeV-range center of mass energies – this would correspond to rates of  $\mathcal{O}(10^2 - 10^5)$  events for an integrated luminosity of  $500 \text{ fb}^{-1}$ .
- **Large quantum effects**, which may reach up to  $\delta_r \equiv [\sigma^{(0+1)} - \sigma^{(0)}]/\sigma^{(0)} \sim \pm 50\%$ , preferably realized within the  $\tan\beta \sim \mathcal{O}(1)$  and  $|\lambda_5| \sim \mathcal{O}(10)$  domains of the 2HDM parameter space. These may alternatively lead to characteristic enhancements (e.g. for  $\sigma(2h)$  at  $\sqrt{s} \simeq 500 \text{ GeV}$ ), or suppressions (for  $\sigma(hZ)$  and also for  $\sigma(2h)$  at larger  $\sqrt{s}$ ).



- **A generic phenomenological pattern**, in the sense that the above observations barely depend on the very choice of Higgs masses nor the type of Yukawa couplings to fermions, and they hold for broad regions across the  $\tan\beta - \sin\alpha$  plane.

Interestingly enough, enhancements of the Higgs boson production rates have also been put forward in the literature for alternative multi-Higgs production processes, such as the  $e^+e^- \rightarrow hhh$  [13] and  $e^+e^- \rightarrow VV^* \rightarrow hh + X$  [14] channels. In this vein, let us consider the following choice of parameters:  $\tan\beta = 1$ ,  $\alpha = \beta$  and  $\lambda_5 = -10$ , along with Set B of Higgs boson masses from Tab. 1. This particular configuration saturates the unitarity bounds, and thus maximizes the impact of the Higgs boson self-interactions. If we now combine the evaluation of the total production rates for all these different production channels, we come up with the cross-correlated set of predictions displayed in Tab. 2. These results reflect the great complementarity of the different multi-Higgs states at different center-of-mass energies. Likewise, the correlation of large negative quantum effects on the Higgs-strahlung channels with the presence of significant positive (for  $\sqrt{s} \lesssim 500$  GeV) and negative (for  $\sqrt{s} > 600$  GeV) quantum effects on the double Higgs production may eventually constitute an additional hint at a generic (unconstrained) 2HDM dynamics. Notice once more that, in all these cases, the reported pattern of signatures crucially relies on the strength of the 3H self-couplings. No analogue picture could then be attributed e.g. to the MSSM.

On balance, there is little doubt that a linear collider qualifies as a most cherished tool to carry to completion the Higgs boson research program. Owing to its superbly clean environment, a linac facility should enable accurate measurements of the Higgs boson masses, gauge and Yukawa couplings, as well as of the Higgs boson self-interactions themselves. This means, it could provide us with the firmest possible grip on the fundamental structure of the EWSB sector. In this context, our results underline the possibilities of the Higgs boson self-interactions as a trademark dynamical feature of the generic 2HDM. We prove their capabilities to rubber-stamp significant – and highly distinctive – fingerprints on multi-Higgs production processes, either at the leading order or through quantum corrections, and conclude that these might well constitute a pristine window towards non-standard, non-supersymmetric Higgs sectors.

## 4 Acknowledgments

DLV wishes to thank the LC2012 local organizing committee and, in particular, Gudrid Moorgat-Pick and Georg Weiglein, for the hospitality extended to him at DESY and also for travel support. JS has been supported in part by MEC and FEDER under project FPA2010-20807, by the Spanish Consolider-Ingenio 2010 program CPAN CSD2007-00042 and by DIUE/CUR Generalitat de Catalunya under project 2009SGR502.

## References

- [1] ATLAS Collaboration, ATLAS-CONF-2011-157; CMS Collaboration, CMS-PAS-HIG-11-03.
- [2] H. Haber, *J. Phys. Conf. Ser.* **G259** (2010) 012017.
- [3] J.F. Gunion, H.E. Haber, G.L. Kane, S. Dawson, *The Higgs hunter's guide*, Addison-Wesley, Menlo-Park, 1990; G. C. Branco et al. arXiv:1106.0034 [hep-ph].
- [4] M. Moretti, F. Piccinini, R. Pittau, J. Rathsmann, *JHEP* 1011 (097) 2010, M. Aoki et al, *Phys. Rev. D* **84**, 055028 (2011) [arXiv:1104.3178 [hep-ph]]; S. Chang, J. A. Evans, M. A. Luty, *Phys. Rev. D* **84** (2011) 095030; S. Kanemura, K. Tsumura, H. Yokoya, arXiv:1111.6089 [hep-ph]; A. Arhrib, C. W. Chiang, D. K. Ghosh, R. Santos, arXiv:1112.5527 [hep-ph]; P. M. Ferreira, R. Santos, M. Sher, J. P. Silva, *Phys. Rev. D* **85**, 035020 (2012); [arXiv:1201.0019 [hep-ph]]; arXiv:1112.3277 [hep-ph]; G. Burdman, C. Haluch, R. Matheus, arXiv:1112.3961 [hep-ph].
- [5] H.P. Nilles, *Phys. Rept.* **110** (1984) 1; H.E. Haber, G.L. Kane, *Phys. Rept.* **117** (1985) 75; S. Ferrara, ed., *Supersymmetry*, vol. 1-2 (North Holland, World Scientific, 1987).
- [6] S. Kanemura, T. Kubota and E. Takasugi, *Phys. Lett.* **B313** (1993) 155; A. Akeroyd, A. Arhrib, E.-M. Naimi, *Phys. Lett.* **B490** (2000) 119. See also Sect. III of Ref. [10].
- [7] M. Sher, *Phys. Rept.* **179** (1989) 273; S. Nie and M. Sher, *Phys. Lett.* **B449** (1999) 89; S. Kanemura, T. Kasai, Y. Okada, *Phys. Lett.* **B471** (1999) 182; P.M. Ferreira, D.R.T. Jones, *JHEP* 08 (2009) 069.
- [8] M. B. Einhorn, D.R.T. Jones, M. J. G. Veltman, *Nucl. Phys.* **B191** (1981) 146.

- [9] F. Mahmoudi, <http://superiso.in2p3.fr>; F. Mahmoudi, *Comput. Phys. Commun.* **178** (2008) 745; *Comput. Phys. Commun.* **180** (2009) 1579.
- [10] D. López-Val, J. Solà, *Phys. Rev.* **D81** (2010) 033003; *Fortsch. Phys.* **G58** (2010) 660; PoS RADCOR2009, 045 (2010).
- [11] A. Wahab El Kaffas, P. Osland, O. M. Greid, *Phys. Rev.* **D76** (2007) 095001; H. Flücher, M. Goebel, J. Haller, A. Höcker, K. Mönig, J. Stelzer, *Eur. Phys. J* **C60** (2009) 543; N. Mahmoudi, O. Stål, *Phys. Rev.* **D81** (2010) 035016; S. R. Juárez, D. Morales, P. Kielanowski, arXiv:1201.1876
- [12] *ILC Reference Design Report Volume 2: Physics at the ILC*, arXiv:0709.1893; G. Weiglein *et al.*, *Physics interplay of the LHC and the ILC.*, *Phys. Rept.* **426** (2006) 47, hep-ph/0410364; H. E. Haber, *A framework for precision 2HDM studies at the ILC and CLIC*, arXiv:1203.2631 [hep-ph].
- [13] G. Ferrera, J. Guasch, D. López-Val, J. Solà, *Phys. Lett.* **B659** (2008) 297; PoS RADCOR2007, 043 (2007), arXiv:0801.3907.
- [14] R. N. Hodgkinson, D. López-Val, J. Solà, *Phys. Lett.* **B673** (2009) 47.
- [15] A. Arhrib, G. Moulhaka, *Nucl. Phys.* **B558** (1999) 3; A. Arhrib, M. Capdequi Peyranère, W. Hollik, G. Moulhaka, *Nucl. Phys.* **B581** (2000) 34; J. Guasch, W. Hollik, A. Kraft, *Nucl. Phys.* **B596** (2001) 66.
- [16] D. López-Val, J. Solà, N. Bernal, *Phys. Rev.* **D81** (2010) 113005; D. López-Val, J. Solà, PoS RADCOR2009, 045 (2010); *Fortsch. Phys.* 58 (2010) 660.
- [17] See e.g. P. Chankowski, S. Pokorski, J. Rosiek, *Nucl. Phys.* **B423** (1994) 437; V. Driesen, W. Hollik, *Zeitsch. f. Physik* **C68** (1995) 485; A. Djouadi, H.E. Haber, P.M. Zerwas, *Phys. Lett.* **B375** (2003) 1996; A. Djouadi, W. Kilian, M. Mühlleitner, P. M. Zerwas, *Eur. Phys. J* **C10** (1999) 27; S. Heinemeyer, W. Hollik, J. Rosiek and G. Weiglein, *Int. J. of Mod. Phys.* **19** (2001) 535; H. E. Logan, S.-f. Su, *Phys. Rev.* **D66** (2003) 035001; E. Coniavitis, A. Ferrari, *Phys. Rev.* **D75** (2007) 015004; O. Brein, T. Hahn, *Eur. Phys. J* **C52** (2007) 397.
- [18] D. L. Borden, D. A. Bauer, D. O. Caldwell, *Phys. Rev. D* **48**, 4018 (1993); P. Niezurawski, A. F. Żarnecki, M. Krawczyk, *Acta Phys. Polon. B* **34**, 177 (2003)
- [19] N. Bernal, D. López-Val, J. Solà, *Phys. Lett.* **B677** (2009) 38.
- [20] D. López-Val, J. Solà, *Phys. Lett.* **B702** (2011) 246; J. Solà, D. López-Val, *Nuovo Cim.* **C34** (2011) 57; D. López-Val, arXiv:1202.1075.
- [21] B. Grzadkowski, J.F. Gunion, *Phys. Lett.* **B294** (1992) 361; J. F. Gunion, H.E. Haber, *Phys. Rev.* **D48** (1993) 5; S.-h. Zhu, C.-s. Li, C.-s. Gao, *Chin. Phys. Lett.* 15 (1998) 2; M. Mühlleitner, M. Krämer, M. Spira, P. Zerwas, *Phys. Lett.* **B508** (2001) 311; D. M. Asner, J. B. Gronberg, J.F. Gunion, *Phys. Rev.* **D67** (2003) 035009; M. Krawczyk, hep-ph/0307314; P. Niezurawski, A.F. Żarnecki, M. Krawczyk, *Acta Phys. Polon. B* 37 (2006) 1187.
- [22] see e.g. F. Cornet and W. Hollik, *Phys. Lett.* **B669** (2008) 58; E. Asakawa, D. Harada, S. Kanemura, Y. Okada and K. Tsumura, *Phys. Lett.* **B672** (2009) 354; A. Arhrib, R. Benbrik, C.-H. Chen, R. Santos, *Phys. Rev.* **D80** (2009) 015010; E. Asakawa, D. Harada, S. Kanemura, Y. Okada, K. Tsumura, *Phys. Rev.* **D82** (2010) 115002.
- [23] J.D. Bjorken, in: proc. of the 1976 SLAC Summer Institute on Particle Physics, ed. M. Zipf (SLAC Report No. 198, 1976) p. 22; D.R.T. Jones and S.T. Petcov, *Phys. Lett.* **B84** (1979) 440.
- [24] T. Hahn, *Comput. Phys. Commun.* 140, 418 (2001); T. Hahn, C. Schappacher, *Com. Phys. Comm.* **G143** (2002) 54; T. Hahn and M. Pérez-Victoria, *Com. Phys. Comm.* **G118** (1999) 153.
- [25] D. Eriksson, J. Rathsmann, O. Stål, *Com. Phys. Comm.* **G181** (2010) 189, <http://www.isv.uu.se/thep/MC/2HDMC/>.
- [26] P. Bechtle, O. Brein, S. Heinemeyer, G. Weiglein, K. E. Williams, *Com. Phys. Comm.* **G181** (2010) 138; arXiv:1102.1898, <http://www.ippp.dur.ac.uk/HiggsBounds>.
- [27] M. Bohm, H. Spiesberger and W. Hollik, *Fortsch. Phys.* **G34** (1986) 87; A. Denner, *Fortsch. Phys.* **G41** (1993) 307.